An Assessment of Wildfire Smoke in Western U.S. National Parks Using IMPROVE Monitoring Data

Keith A. Rose, Environmental Scientist
Environmental Protection Agency, Region 10
karose30@gmail.com

I. Introduction

Increased forest fire activity across the western continental United States in recent decades has been associated with a number of factors, including the legacy of fire suppression and human settlement, natural climate variability, and human-caused climate change (Abatzoglou and Park, 2016). These authors used modeled climate projections to estimate the contribution of anthropogenic climate change to observed increases in eight fuel aridity metrics and forest fire area across the western U.S. They found that anthropogenic contribution to climate change significantly enhanced fuel aridity across western U.S. forests over the past several decades. The authors estimated that human-caused climate change contributed to an additional 4.2 million hectares of forest fire area burned in the western U.S. during 1984–2015, nearly doubling the forest fire area expected in its absence.

In a paper by Dennison et. al., the authors used burn area boundaries mapped from satellite remote sensing data by the Monitoring Trends in Burn Severity Project (MTBS) to determine wildfire trends within nine ecoregions spanning the western U.S. The MTBS database captures large wildfires (> 405 hectares) in the western U.S. to document regional trends in fire occurrence, total fire area, fire size, and day of year of ignition for 1984–2011. Over the western U.S. and in a majority of western ecoregions, the authors found significant, increasing trends in the number of large fires and/or total large fire area per year. Trends were most significant for southern and mountain ecoregions, coinciding with trends toward increased drought severity in those ecoregions. The authors concluded that the geographically broad and coherent nature of fire and climate trends across much of the study area implicated climate as a dominant driver of changing fire activity in the western U.S.

This study used Positive Matrix Factorization (PMF), a multivariate factor analysis tool that decomposes a matrix of speciated sample data into a factor contributions matrix and a factor profiles matrix, to identify wildfire smoke contributions to $PM_{2.5}$ mass measured at IMPROVE monitors in six western U.S national parks. PMF was used to identify smoke contributions over two 5-year time periods separated by approximately 20 years. These results were then used to determine if there has been a significant change in wildfire smoke contributions at each site between the two time periods.

II. Methods

1. Chemically Speciated $PM_{2.5}$ Data

Chemically speciated $PM_{2.5}$ data were obtained from the IMPROVE Network. The IMPROVE monitoring program began in 1988 and its monitors collect 24-hour $PM_{2.5}$ samples that are analyzed for ions (sulfates and nitrates), organic and elemental carbon, and total mass. The organic and elemental carbon components consist of organic carbon fractions OC1-OC4 and elemental carbon fractions EC1-EC3. These monitors collect samples once every third day on an annual basis. Information about the IMPROVE network can be found on the IMPROVE web site (http://vista.cira.colostate.edu/improve/).

2. IMPROVE Monitoring Sites Selected

The IMPROVE monitoring sites selected for this study were six national parks in the western U.S that represent diverse ecoregions of the West. Sites were selected for PMF analysis if they had at least 90% complete data for the two 5-year time periods. The first 5-year period was in the early 1990's, and the second 5-year period began in the late 2000s. The exact 5-year time period for each site varied slightly within these two time periods depending on the completeness of the data at each site. The six national parks chosen were Mt. Rainier, Yosemite, Yellowstone, Glacier, Rocky Mountain, and Grand Canyon. The monitoring sites chosen for this study and their locations are shown in Table 1.

3. Data Preparation

IMPROVE datasets were processed to correct for missing or negative values and incomplete data. Dates with substantial missing data or missing total fine mass values were eliminated, and chemical species with more than 50% missing data were eliminated. Any negative concentrations were reset to zero. PMF replaced all missing data values with species median concentrations, and the associated uncertainty was set to four times the species median concentration to minimize the influence of the replaced data on the model solution. The signal-to-noise (S/N) ratio function of PMF was also used to evaluate whether chemical species should be included in the modeling, and was used to adjust the data uncertainty. Species were omitted in PMF modeling if the S/N ratio was less than 0.5, and for species with S/N between 0.5 and 1.0, data uncertainties were multiplied by a factor of three to down-weight the influence of these species in the model solution (Norris et al., 2014). For chlorine, measured in the IMPROVE network by both elemental (Cl) and ion analyses (Cl-), Cl- data was used to avoid double counting. Also, since the reported lowest temperature fraction of EC, EC1, is actually the sum of pyrolyzed organic carbon (OP) and EC1, EC1 was recalculated as EC1-OP.

4. Source Apportionment with PMF

Source apportionment modeling was performed using EPA PMF 5.0 (Norris et al., 2014). A discussion of the mathematical equations underlying EPA PMF can be found in Paatero and Hopke (2003) and Norris et al. (2014). PMF uses both sample concentration and uncertainty associated with the sample data to weight individual data points. EPA PMF 5.0 requires multiple iterations of the underlying Multilinear Engine to help identify the optimal factor contributions and profiles. PMF generates a best-fit solution for an operator-selected number

of factors. Factor contributions and profiles are derived by the PMF model by minimizing the objective function "*Q*", also known as the goodness-of-fit parameter.

Data from each monitoring site was modeled independently, and PMF was run in the robust mode with 40 repeat runs to ensure the model least-squares solution represented a global, rather than local minimum. As recommended in the PMF 5.0 User's Guide (Norris et al., 2014), 100 Bootstrap runs were performed to ensure the robustness of the statistics. In running PMF, fine mass was set as the total variable, and the model solution with the optimum number of factors was determined by the following process. First, the data from each site was analyzed by PMF for solutions of 4 to 7 factors, and the resulting PMF profiles were identified by comparing them to profiles in EPA's SPECIATE database (https://cfpub.epa.gov/speciate/), comparing them to identified PMF profiles in existing published studies, and knowledge of the seasonal emissions patterns of natural aerosol sources (e.g., wildfire smoke and wind-blown dust). Second, the PMF solutions were evaluated with the "bootstrap" error estimation method in PMF, one of the three error estimation methods available in PMF 5.0. Based on the recommendation in the EPA PMF 5.0 Users Guide, a bootstrap match of at least 80% was used to determine if a solution was acceptable. Finally, the PMF solution which contained the maximum number of identifiable sources (factors), and had at least 80% bootstrap match, was evaluated by all three error estimation methods, "bootstrap", "displacement", and "bootstrapping with displacement" to determine if there were any swaps in "best fit" (Norris et al., 2014). If swaps were observed at this level, the PMF solution with the next lower number of factors was evaluated. In this way, the optimal solution was found to be the one which had the highest number of identifiable sources and which had no swaps in best fit.

III. Results

1. PMF Factors and Association Sources

Seven different PMF factors and associated sources were identified in this study.

a. PMF Factor Associated with Ammonium Sulfate

The main chemical species in this factor was sulfate and was assumed to be fully neutralized by ammonium. This factor typically had a seasonal pattern of high concentrations in the summer months and low concentrations during the winter. This factor was identified at all six sites. A composite ammonium sulfate profile is shown in Figure 1.

b. PMF Factor Associated with Ammonium Nitrate

The main chemical constituent in this factor was nitrate and was assumed to be fully neutralized by ammonium. This factor typically had a seasonal pattern of high concentrations in the winter and spring months but low concentrations in the summer. This factor was identified at all six sites, and a composite ammonium nitrate profile is shown in Figure 2.

c. PMF Factor Associated with Wildfire/Wood Smoke

The dominant chemical species in this factor was OC3, with substantial amounts of OC2, OC4 and OP. These four species made up about 80% of the mass associated with this profile. Also present in this profile were significant amounts of EC1 and EC, and trace amounts of potassium. The time series for this factor showed peaks in mid to late summer

and had episodic spikes in the range of 8-20 μg/m3 at all sites. This factor was identified at all six sites, and a composite wildfire/wood smoke profile is shown in Figure 3.

d. PMF Factor Associated with Motor Vehicles

This factor contained substantial amounts of EC1, OC2, OC3, OC4, and sulfate, a moderate amount of nitrate, and trace amounts of iron, zinc, lead, silicon, and copper. The dominant chemical constituents are similar to those found for motor vehicles in previous publications (Kotchenruther, 2017; Kim and Hopke, 2006; Hwang and Hopke, 2007). Separate factors for gasoline and diesel vehicles were not found in this study, so this factor represents a combination of these two sources. This factor was identified at all sites except Yellowstone and Glacier National Parks. A composite motor vehicle profile for all sites, except Yellowstone and Glacier, is shown in Figure 4.

e. PMF Factor Associated with Sea Salt

This factor was dominated by sodium, chlorine, and sulfate and included trace amounts of magnesium, calcium, and potassium. Contributions from this factor occurred primarily in the winter and spring months suggesting this factor was due to marine air intrusions. This factor was only clearly identified at the Mt. Rainer site, and the sea salt profile for Mt. Rainier is shown in Figure 5. At the Yosemite site the sea salt profile had a smaller chlorine concentration and larger nitrate and sulfate concentrations, and is representative of aged sea salt. The replacement of chlorine with nitrate is typical of aged sea salt (Adachi and Buseck, 2015).

f. PMF Factor Associated with Soil/Crustal Material

The dominant chemical species in this factor were silicone, aluminum, calcium, iron, and sulfate. These five species constituted about 80% of mass associated with this profile. This profile also contained smaller amounts of potassium and magnesium. The contribution from this source was high from late spring through summer and lower in fall and winter. This factor was identified at all six sites, and a composite soil profile is shown in Figure 6.

g. Iron-rich PMF Factor

This factor was dominated by EC1, OC2, OC3, OC4, and iron. Also present were smaller amounts of silicone and nitrate. This factor was identified only at the Glacier National Park site, and contributed to that site at a relative constant rate, showing no seasonality. It is likely this factor is related to steel foundries, steel manufacturing, or other metal fabrication facilities in southern Alberta, Canada. The profile for this factor is shown in Figure 7.

2. Analysis of Wildfire Smoke Contribution between Time Periods

The average source contributions for all sources impacting each monitoring site over each 5-year time period are shown in Table 2. As can be seen from this table, average smoke concentrations are the highest of any average source concentration at all sites, and the average smoke concentrations increased between time periods in the Rocky Mountain and Yellowstone National Parks.

To determine if the distribution of smoke contributions from the two time periods at each site were significantly different, the smoke contributions at each site were evaluated with

Levene's test, a nonparametric test for variance in two or more populations. Levene's tests were performed with an Excel macro (QI Macros, https://www.qimacros.com/). The results of this test showed that there is a significant difference in variance ($p = 0.05$) in the distribution of smoke concentrations between the two time periods at Grand Canyon, Mt. Rainier, Rocky Mountain, and Yellowstone National Parks.

To observe how the distributions of smoke contributions differ between the two time periods for the four sites which had a significant difference in variance according to Levene's test, the smoke concentrations for these four sites were plotted as a function of percentile ranking. Figure 8 shows that the smoke concentrations in the 90-100 percentile range at the Grand Canyon were greater for 2009-2013 than for 1993-1997, and the maximum concentration for 2009-2013 was approximately 3.8 times the maximum concentration for 1993-1997. Figure 9 shows that the smoke concentrations in the 70-100 percentile range at Mt. Rainier were greater for 2008-2012 than for 1992-1996, and the maximum concentration for 2008-2012 was approximately 1.2 times the maximum concentration for 1992-1996. Figure 10 shows that the smoke concentrations in the 70-100 percentile range at Rocky Mountain were greater for 2008-2012 than for 1990-1994, and the maximum concentration for 2008-2012 was approximately 1.7 times the maximum concentration for 1990-1994. Figure 11 shows that the smoke concentrations in the 90-100 percentile range at Yellowstone were greater for 2011-2015 than for 1992-1996, and the maximum concentration for 2011-2015 was approximately 5.0 times the maximum concentration for 1992-1996.

IV. Conclusions

The results of this study show that there has been an increase in smoke concentrations in the higher percentile ranges in the last two decades in the Grand Canyon, Mt. Rainier, Rocky Mountain, and Yellowstone National Parks, representing four western ecoregions (the central Cascades, the south central Rockies, the Colorado Rockies, and the Arizona Plateau). These results support the observation by Dennison et. al. that the number of large fires and/or total large fire area burned per year has increased over the western U.S. and in a majority of western ecoregions since the 1980s.

Although wildfires are a natural part of most western forest ecosystems, warmer and drier conditions have helped increase the number and extent of wildfires in western U.S. forests since the 1970s. This trend is expected to continue under future climate conditions predicted by modeling. For example, by the 2080s the median annual area burned in the Northwest could quadruple, relative to the 1916 to 2007 period, to about 2 million acres under the A1B global greenhouse gas emission scenario (Littell, et. al., 2010).

It is also well documented that exposure to smoke from wildfires increases the number of hospitalizations and medical visits associated with health issues like asthma, bronchitis, respiratory infections, and lung illnesses (Dennekamp and Abramson, and Defino et. al.). If wildfires in the western U.S. increase as predicted, wildfire smoke in western national parks over the next several decades will further impact the health of visitors that are susceptible to

respiratory diseases. Also, increased smoke concentration during extreme episodic wildfire events will further reduce visibility in western national parks and wilderness areas on the days impacted by these events.

Table 1. Locations of IMPROVE Monitoring Sites

National Park	State	Code	Time Period	Latitude	Longitude
Glacier	MT	GLAC1	1988-2015	48.5105	-113.9966
Grand Canyon #1	AZ	GRAC1	1988-1998	36.0658	-112.1539
Grand Canyon #2	AZ	GRAC2	1996-2015	35.9731	-111.9841
Mt. Rainier	WA	MORA1	1988-2015	46.7583	-122.1244
Rocky Mt.	CO	ROMO1	1990-2015	40.2783	-105.5457
Yellowstone #1	WY	YELL1	1988-1996	44.5654	-110.4003
Yellowstone #2	WY	YELL2	1996-2015	44.5653	-110.4002
Yosemite	CA	YOSE1	1988-2015	37.7133	-119.7061

Figure 1- Composite Sulfate Profile

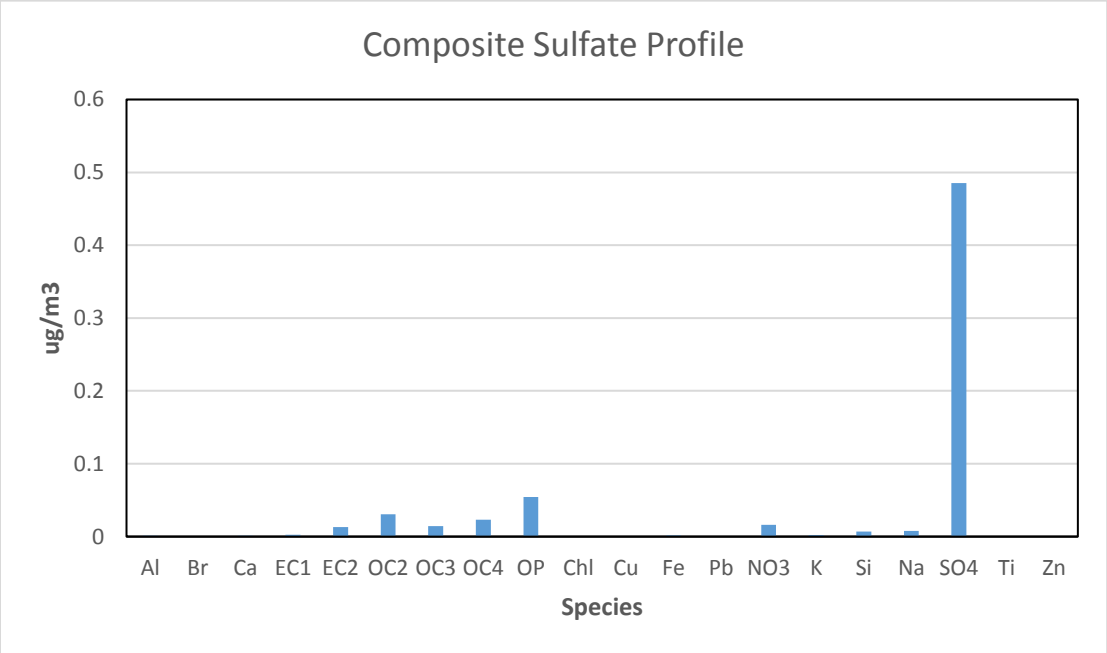

Figure 2. Composite Nitrate Profile

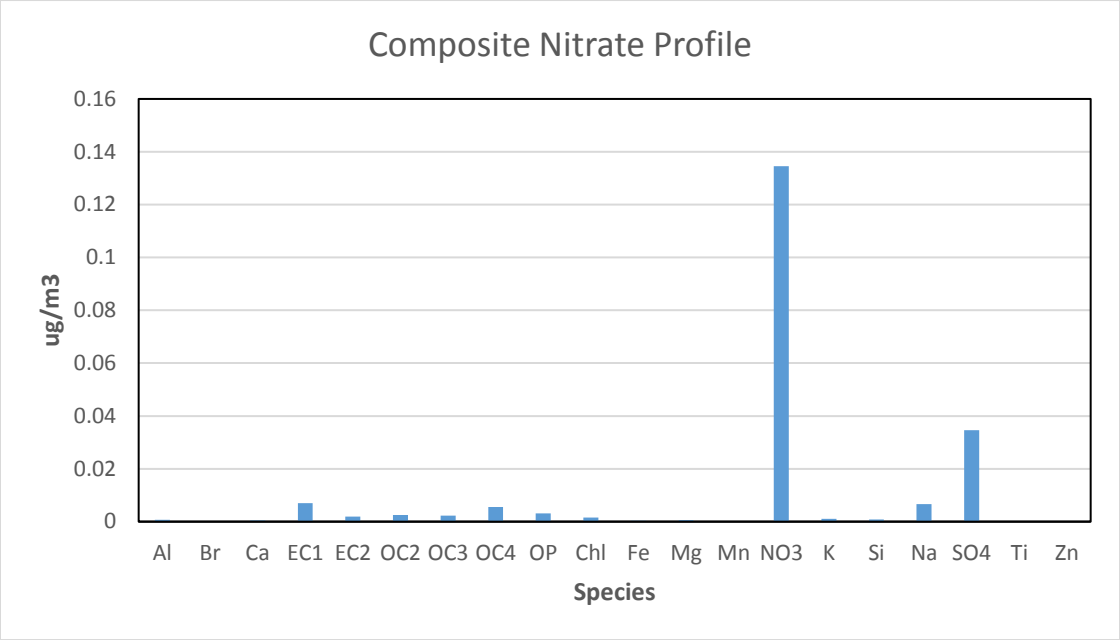

Figure 3. Composite Wildfire/Wood Smoke Profile

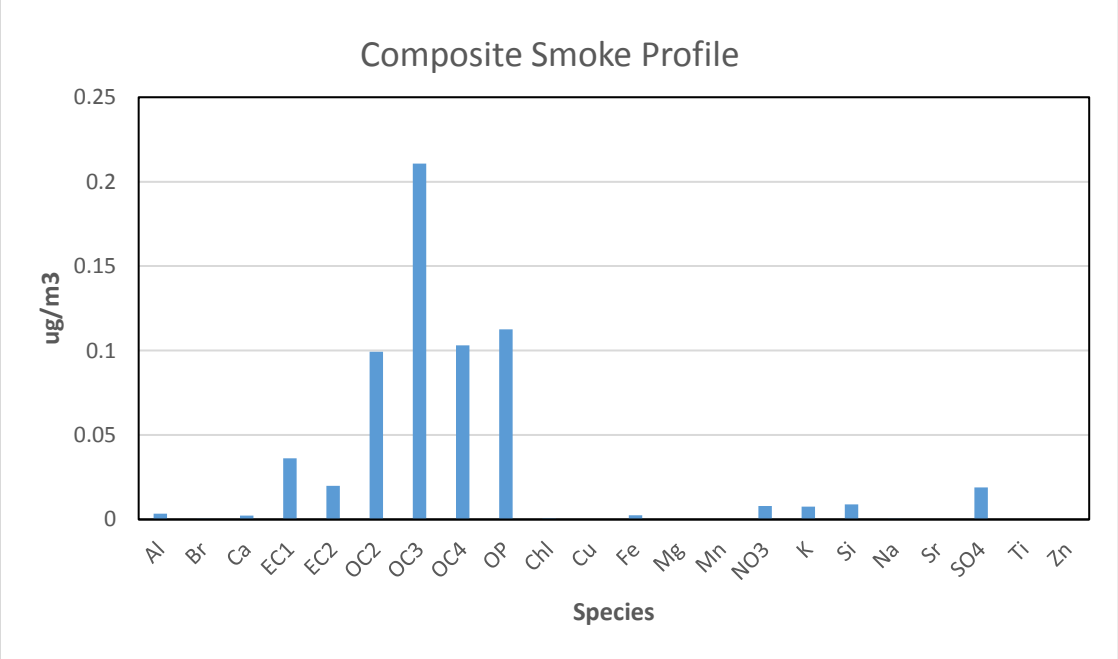

Figure 4. Composite Motor Vehicle Profile

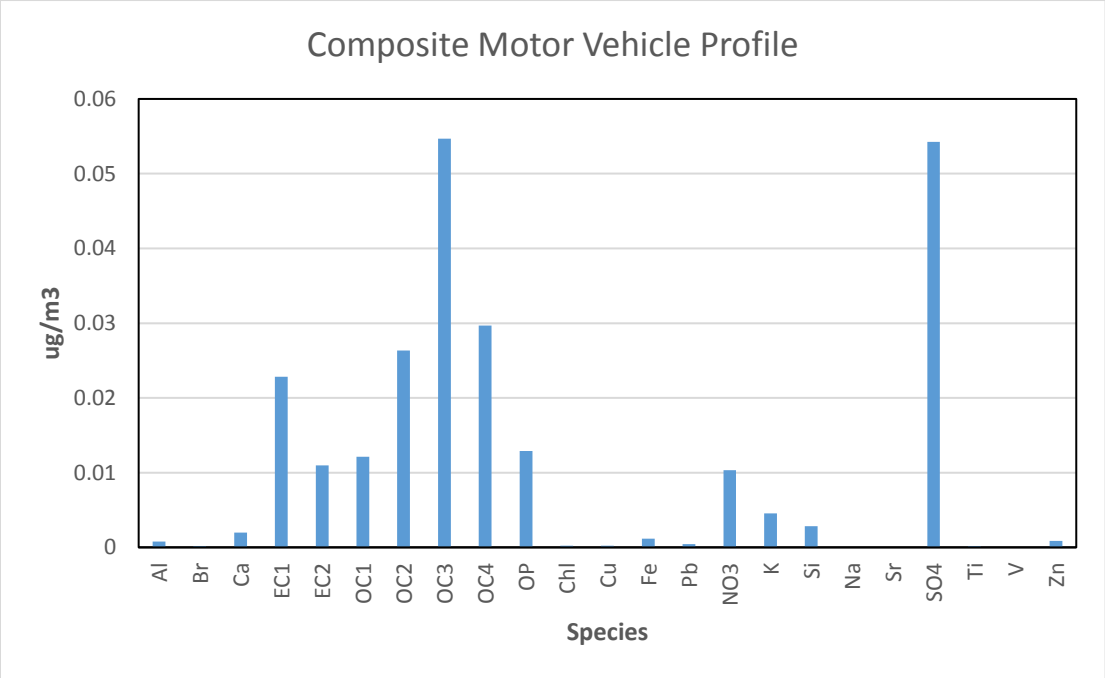

Figure 5. Mt. Rainier National Park Sea Salt Profile

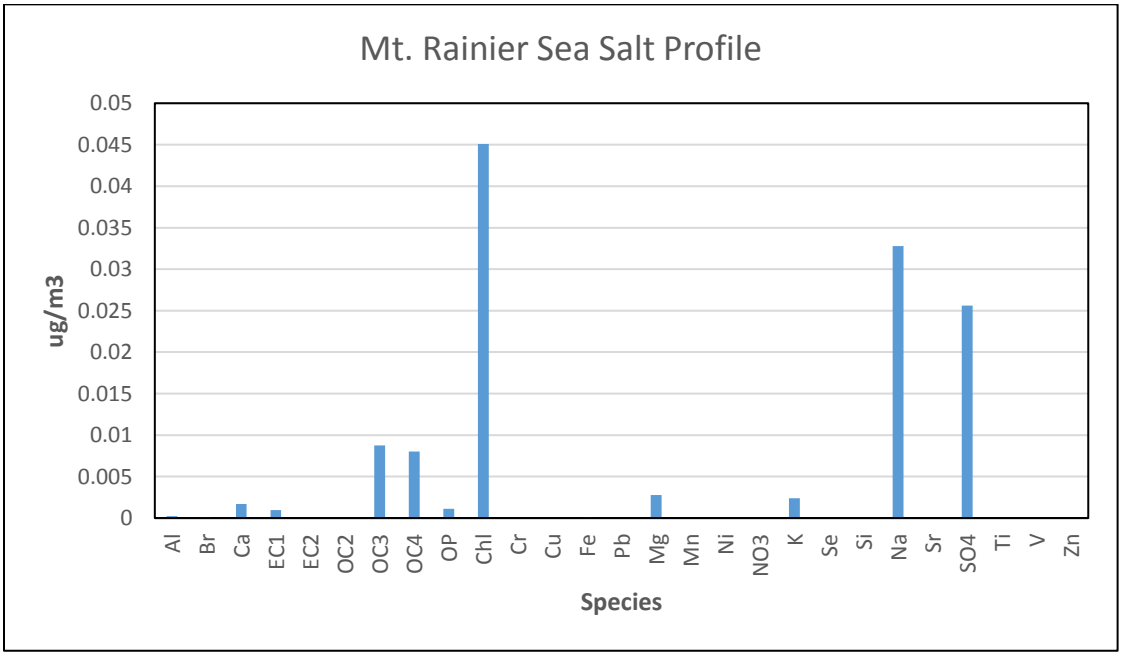

Figure 6. Composite Soil Profile

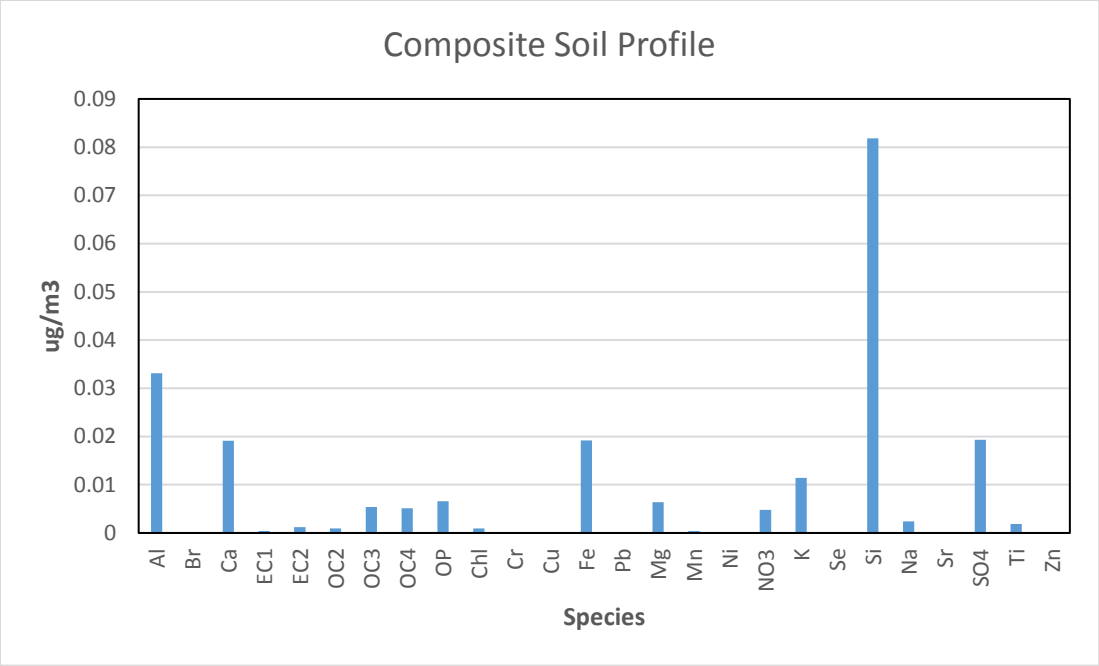

Figure 7. Glacier National Park Iron Rich Profile

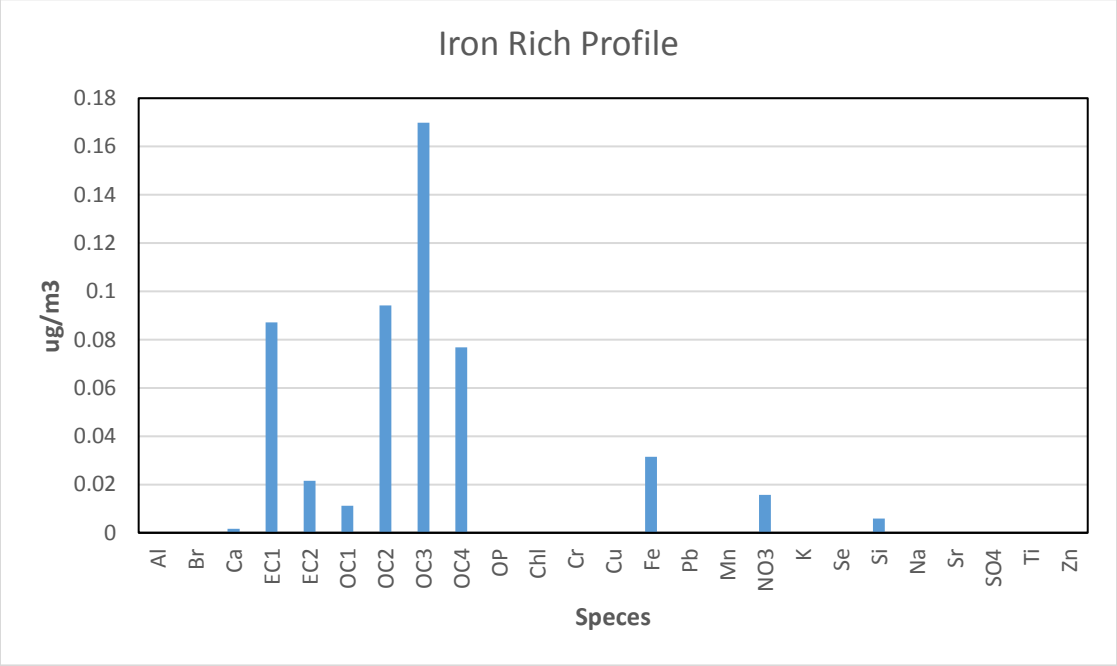

Table 2. Average Source Contribution for each Time Period ($\mu g/m^3$)

Site	Years	Smoke	SO4	NO3	Soil	Mobile	Marine	Fe-rich
Glacier	1992-96	2.194	1.301	0.440	0.647			0.806
	2008-12	1.779	0.779	0.171	0.526			0.478
Grand Canyon	1993-97	0.917	1.110	0.193	0.622	0.233		
	2009-13	0.886	0.706	0.130	0.633	0.411		
Mt. Rainier	1992-96	1.571	1.134	0.678	0.488	1.071	0.176	
	2008-12	1.139	0.661	0.103	0.205	0.458	0.203	
Rocky Mt.	1990-94	0.956	1.067	0.224	0.744	0.305		
	2008-12	1.191	0.447	0.177	0.568	0.278		
Yellowstone	1992-96	1.263	0.741	0.046	0.915			
	2011-15	1.494	0.533	0.082	0.403			
Yosemite	1990-94	1.938	0.842	0.460	0.396	0.329	0.588	
	2011-15	1.675	0.870	0.121	0.382	0.419	0.379	

Figure 8. Ranking of Grand Canyon Smoke Concentrations

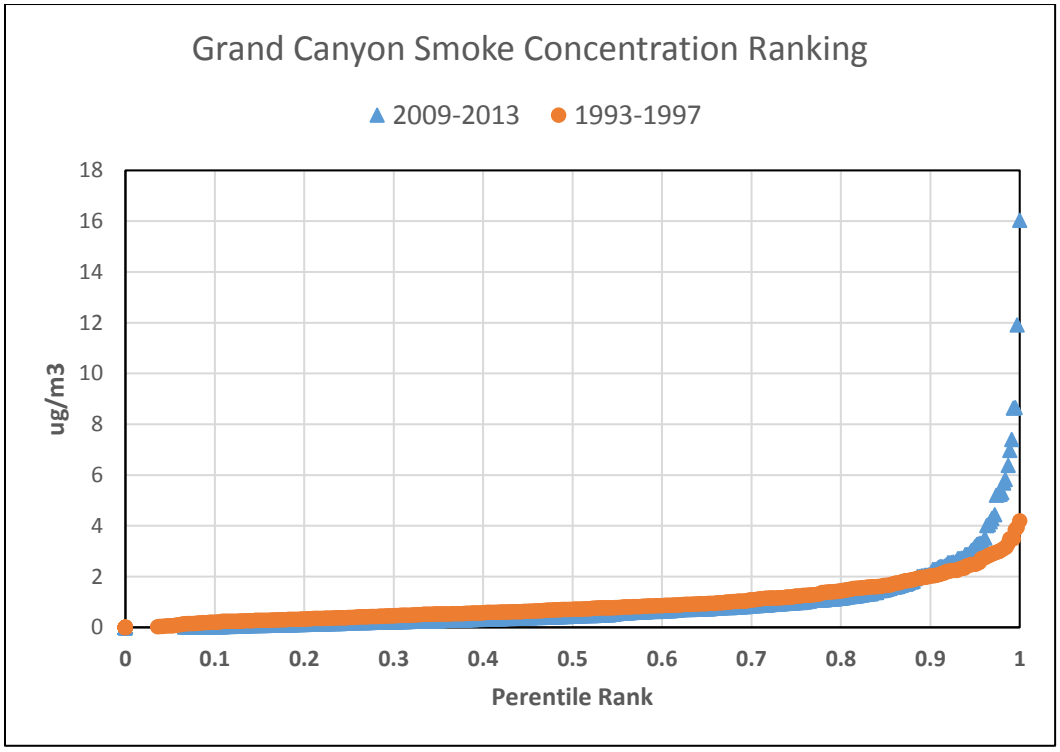

Figure 9. Ranking of Mt. Rainier Smoke Concentrations

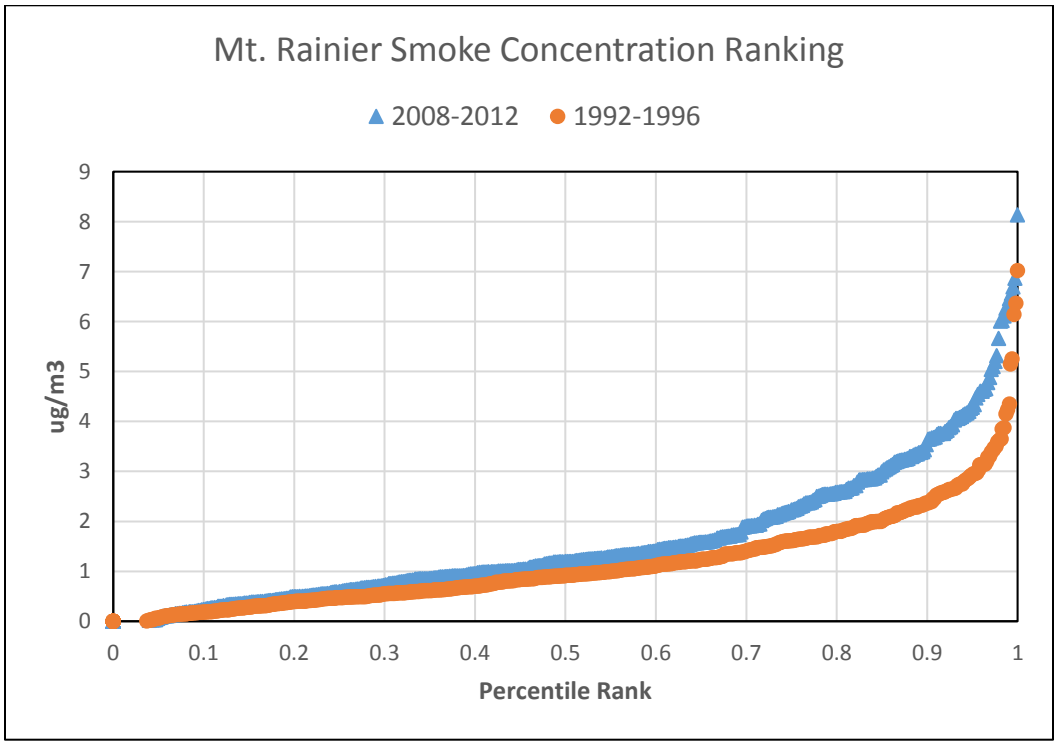

Figure 10. Ranking of Rocky Mt. Smoke Concentrations

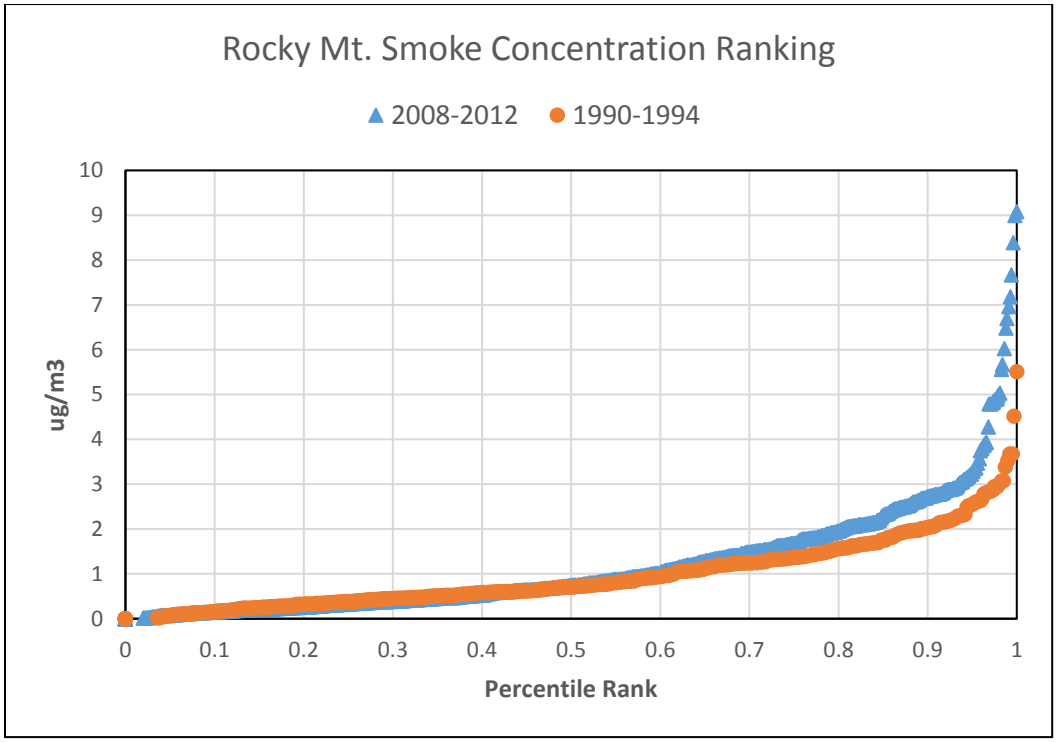

Figure 11. Ranking of Yellowstone Smoke Concentrations

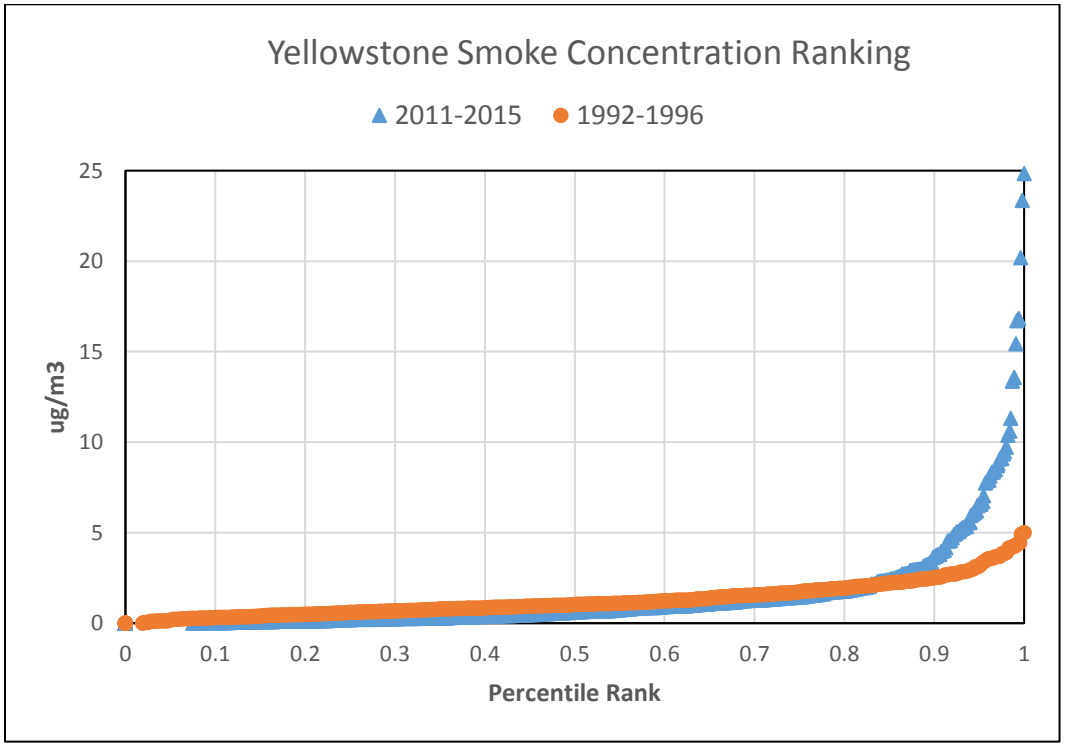

References

Abatzoglou, John T., and A. Park Williams, 2016: Impact of anthropogenic climate change on wildfire across western US forests. Proceedings of the National Academy of Science, vol. 113 no. 42, 11770-11775.

Adachi, K., Buseck, P.R., 2015. Changes in shape and composition of sea-salt particles upon aging in an urban atmosphere. Atmos. Environ. 100, 1-9.

Delfino RJ, Brummel S, Wu J, et. al. The relationship of respiratory and cardiovascular hospital admissions to the southern California wildfires of 2003. Occupational and Environmental Medicine 2009; 66:189-197.

Dennekamp, Martine and Michael J. Abramson: The effects of bushfire smoke on respiratory health. *Respirology* (2011) 16, 198–209.

Dennison, P. E., S. C. Brewer, J. D. Arnold, and M. A. Moritz (2014), Large Wildfire Trends in the western United States, 1984–2011, Geophys. Res. Lett., 41, 2928–2933.
Norris, G., Duvall, R., Brown, S., Bai, S., 2014. EPA Positive Matrix Factorization (PMF) 5.0 Fundamentals and User Guide. U.S. Environmental Protection Agency. EPA/600/R-14/108.

Hwang, I., Hopke, P.K., 2007. Estimation of source apportionment and potential source locations of PM2.5 at a west coastal IMPROVE site. Atmos. Environ. 41, 506-518.

Kim, E., Hopke, P.K., 2006. Characterization of fine particle sources in the Great Smoky Mountains area. Sci. Total Environ. 368, 781-794.

Kotchenruther, R.A., 2017. The effects of marine vessel fuel sulfur regulations on ambient PM2.5 at coastal and near coastal monitoring sites in the U.S. Atmos. Environ. 151, 52-61.

Littell, Jeremy S., Donald McKenzie, David L Peterson, and Anthony L. Westerling: Climate and wildfire area burned in western U.S. ecoprovinces, 1916–2003. Ecological Applications, 19(4), 2009, pp. 1003–1021.

Littell, J. S., E. E. Oneil, D. McKenzie, J. A. Hicke, J. A. Lutz, R. A. Norheim, and M. M. Elsner, 2010: Forest ecosystems, disturbance, and climatic change in Washington State, USA. *Climatic Change*, **102,** 129-158.

Paatero, P., Hopke, P.K., 2003. Discarding or downweighting high-noise variables in factor analytic models. Anal. Chim. Acta 490, 277-289.